Title	Validation of the ohmic, neutral beam and bootstrap currents in non-inductive scenarios at ASDEX Upgrade
Authors	Fischer, R.;Bock, A.;Fable, E.;Giannone, L.;Hobirk, J.;McCarthy, Patrick J.;Rittich, D.;Stober, J.;Tardini, G.;Weiland, M.;Zohm, H.
Publication date	2017-06
Original Citation	Fischer, R., Bock, A., Fable, E., Giannone, L., Hobirk, J., McCarthy, P., Rittich, D., Stober, J., Tardini, G., Weiland, M., Zohm, H. (2017) 'Validation of the ohmic, neutral beam and bootstrap currents in non-inductive scenarios at ASDEX Upgrade', 44th European Physical Society Conference on Plasma Physics 2017. Belfast, Northern Ireland, 26-30 June.
Type of publication	Conference item
Link to publisher's version	http://ocs.ciemat.es/EPS2017PAP/pdf/P4.133.pdf
Rights	© 2017, the Authors. This is an open-access paper distributed under the terms of the Creative Commons Attribution 3.0 Unported (CC BY 3.0) license. - https://creativecommons.org/licenses/by/3.0/
Download date	2025-07-26 06:53:07
Item downloaded from	https://hdl.handle.net/10468/8195

Validation of the ohmic, neutral beam and bootstrap currents in non-inductive scenarios at ASDEX Upgrade

<u>R. Fischer</u>[1], A. Bock, E. Fable, L. Giannone, J. Hobirk, P.J. McCarthy, D. Rittich,

J. Stober, G. Tardini, M. Weiland, H. Zohm, and the ASDEX Upgrade Team

[1]*Max-Planck-Institut für Plasmaphysik, Boltzmannstr. 2, D-85748 Garching, Germany*

Steady-state operation of tokamaks has to rely on a large bootstrap current (I_{BS}) fraction together with substantial current drive from, e.g., neutral heating beams (I_{NBCD}) and microwave heating (I_{ECCD}). Ideally, the inductive voltage induced by the central solenoid is switched off. Uncertainties in the prediction of I_{BS} and the driven currents I_{NBCD} and I_{ECCD} might have an impact on the design and performance of next generation fusion devices. The present work aims at an experimental validation of the predicted contributions from I_{BS}, I_{NBCD} and I_{ECCD} employing ohmic and non-inductive plasmas at ASDEX Upgrade. Since the ohmic current in present-day non-inductive plasmas with large contributions from driven currents is small, non-inductive plasmas provide a scenario where small variations in the predicted ohmic current, loop voltage, and diamagnetic flux can sensitively be compared to evaluations from equilibrium reconstructions. The equilibrium reconstruction couples an *interpretive* Grad-Shafranov equilibrium (GSE) solver with the *predictive* current diffusion equation (CDE) [1]. An extended set of measurements constraining the equilibrium [2] is complemented by flux-surface-averaged toroidal current distributions obtained by solving the CDE between successive equilibria.

To validate various methods for calculating the ohmic current I_{ohm} an ohmic plasma (#33692, $I_{\text{pl}} = 1.0$ MA) is chosen. A first method (M1) is given by the current balance $I_{\text{ohm}} = I_{\text{pl}} - I_{\text{BS}} - I_{\text{NBCD}} - I_{\text{ECCD}}$. For the ohmic plasma I_{BS} is relatively small and $I_{\text{NBCD}} = I_{\text{ECCD}} = 0$ (fig. 1). Further methods to evaluate the ohmic current within a flux surface ρ are given by

Figure 1: *Bootstrap and ohmic current evaluated with 2 different methods and different Z_{eff} values.*

$$I_{ohm}(\rho) = \frac{J(\rho)}{R_0} \int_0^\rho \sigma_\parallel \frac{\tilde{\rho}}{J^2} \frac{\partial \psi}{\partial t}\Big|_{\tilde{\rho}} \, d\tilde{\rho}$$

where $\psi(t)$ can either be determined by integrating the CDE to obtain $\psi_{\text{CDE}}(t)$ (M2) or by solving the GSE $\psi_{\text{GSE}}(t)$ for various time points (M3). Methods (M1) and (M2) coincide (see fig. 3 lower panel) because both are calculated from
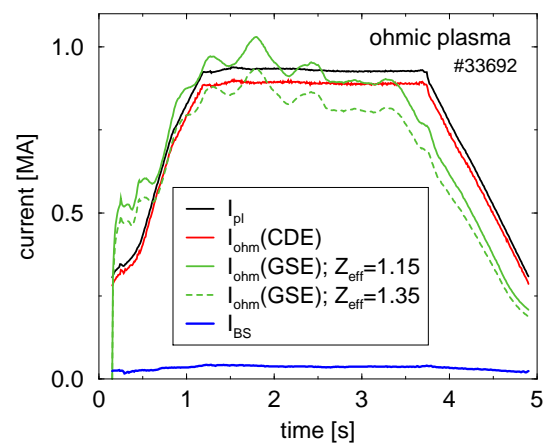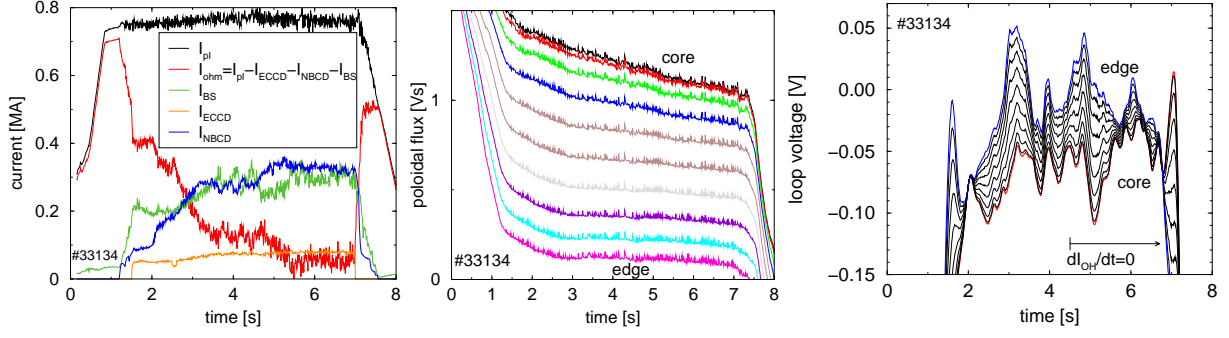
Figure 2: *Time traces of the current mixture (left), of the poloidal flux at various flux surfaces from the core to the edge (middle), and of the loop voltage profile (right).*

results of the CDE, which allows to validate the results of the CDE. Figure 1 shows good agreement between the methods (M2) and (M3) although (M3) depends significantly on Z_{eff}. The first (second) stationary part of the discharge is reasonable described with $Z_{\text{eff}} = 1.35$ (1.15), respectively. Here a variation in Z_{eff} of 20% results in a 10% variation in the evaluated ohmic current using (M3). I_{BS} also depends on Z_{eff} but less pronounced, which, in combination with the small I_{BS} contribution, results in a very small variation of I_{ohm} due to Z_{eff} using (M2).

In contrast to the ohmic plasma with maximum ohmic fraction, non-inductive plasmas are expected to have much reduced ohmic current. Non-inductive improved H-mode operation in ASDEX Upgrade (#33134, $I_{\text{pl}} = 0.8$ MA, $q_{95} \approx 5.3$ and $\beta_{\text{N}} = 2.7$) aims at elevated central q-profiles using ECCD and NBCD with simultaneous large pressure gradients. This can not only improve the stability and confinement of the plasma by eliminating some of the most common resistive MHD instabilities, but also increase the pulse length by increasing the core I_{BS}. The bootstrap fraction of #33134 is about 40%. A fully non-inductive plasma is obtained at $t = 4.5$ s where the current in the central solenoid I_{OH} is fixed. The ohmic current is not vanishing instantaneously as I_{pl} decreases by 20 kA for about 2 s which can also be seen in the decay of the poloidal flux in the center of the plasma. Figure 2 shows the temporal evolution of the current mixture
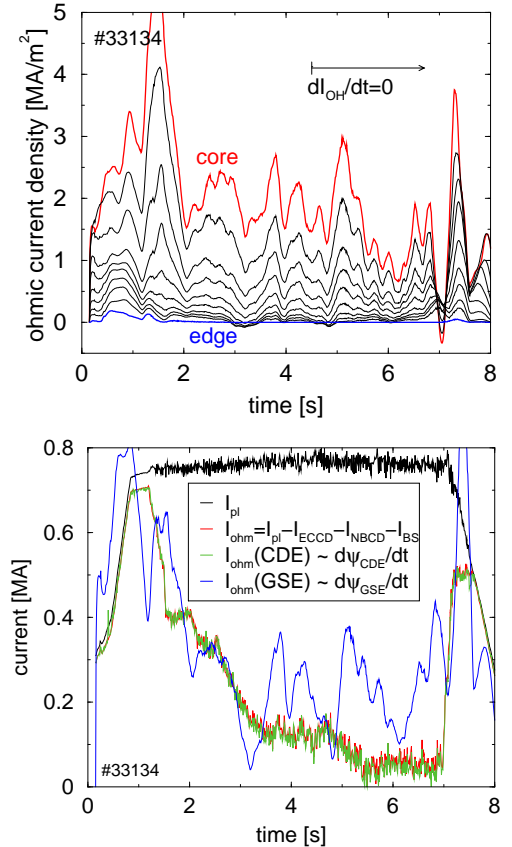

Figure 3: *Time traces of ohmic current density profile and the current mixture.*

(left), of the poloidal flux at various flux surfaces from the core to the edge (middle), and of the loop voltage profile (right). Switching off the central solenoid I_{OH} caused a small accidental

current overshoot, which induced a loop voltage excursion. This loop voltage excursion relaxes within about 1 s in $t = 4.5 - 5.5$ s as can be seen in the loop voltage profile (fig. 2). For $t > 5.5$ s the loop voltage profile is flat but non-zero as one would expect for a stationary plasma where the current is completely driven by external sources and the bootstrap current.

The switching and current relaxation process can also be seen in the profile of the ohmic current density (fig. 3). Although the density is largest in the core, the ohmic current is approximately uniformly distributed (not shown) due to the increase of the poloidal differential area of the flux surfaces with minor radius ρ. The lower panel of figure 3 shows the temporal evolution of I_{ohm} evaluated with (M1)-(M3) where I_{ohm} evaluated with (M3) (blue line) has to be temporally smoothed due to ELM induced noisy distortions of the flux surfaces. In $t = 1 - 3$ s the three methods agree reasonable well. In $t = 3 - 4.5$ s the mean of $I_{\mathrm{ohm}}(GSE)$ (M3) is somewhat larger than $I_{\mathrm{ohm}}(CDE)$ (M2) but the difference is in the order of the fluctuations. For $t > 4.5$ s the mean of $I_{\mathrm{ohm}}(GSE)$ stays approximately constant whereas $I_{\mathrm{ohm}}(CDE)$ is decreasing due to an increase of the calculated I_{NBCD} (fig. 2). At $t > 4.5$ s a (3,2) NTM appears with a presumable decrease of the fast particle population which is not properly considered in the evaluation of the fast particle losses with the TRANSP code. This can also be seen in a discrepancy of the measured and modelled diamagnetic flux in the presence of the NTM [3]. Therefore, it appears reasonable to conclude that the ohmic current $I_{\mathrm{ohm}}(GSE)$ calculated with (M3) is reliable whereas the ohmic current from the current balance (please note that (M1) and (M2) are from the same CDE modelling) is misleading due to a possible overestimation of I_{NBCD}.

In order to identify candidates for the residual discrepancy between $I_{\mathrm{ohm}}(CDE)$ and $I_{\mathrm{ohm}}(GSE)$ in $t = 3 - 4.5$ s, the effects of errors in Z_{eff}, the bootstrap current model, the trapped particle fraction and I_{ECCD} are studied. Different models for the trapped particle fraction f_{t} resulted in minor variations of I_{BS}. Compared to the simple approach $f_{\mathrm{t}} = \sqrt{1 - r_{\min}/r_{\max}}$ the fairly accurate model of [4] gives a reduction in I_{BS} of only 1-2%. Similarly, errors in I_{ECCD} are insignificant due to its small contribution to the current mixture. To identify errors in modelling of I_{BS}, the Sauter model [5] is compared to a recent modification by Hager [6]. Figure 4 compares the contributions of the T_{e}, T_{i},
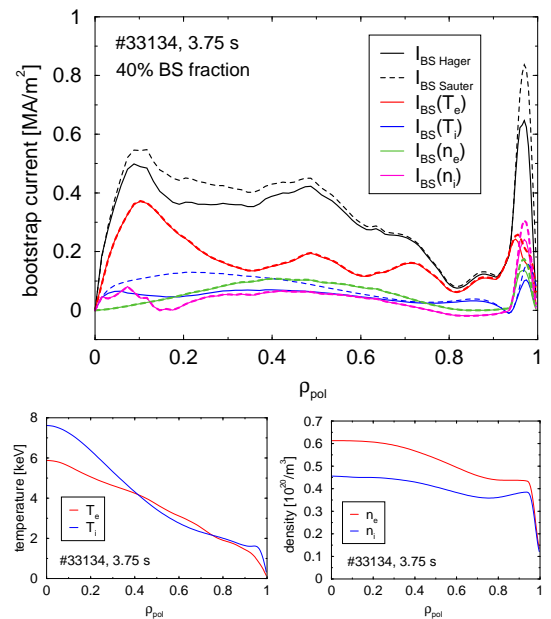
Figure 4: *Bootstrap current profile and its constituents calculated with the Sauter formula and a recent modification, and the kinetic profiles used.*

n_e and n_i profiles to the bootstrap current densities $I_{BS,Sauter}$ and $I_{BS,Hager}$. The fast ion density $n_{i,fast}$ is subtracted from n_i which makes the logarithmic gradients of n_e and n_i different. It is assumed that the fast ion contribution to the current is completely included in I_{NBCD}. The main differences in I_{BS} from the two approaches are in the amplitude of the edge bootstrap peak of all constituents and the core contribution from the T_i-profile. Using the improved approach [6] decreases I_{BS} in $t = 3 - 4.5$ s by about 20% which results in a reduced discrepancy between $I_{ohm}(CDE)$ and $I_{ohm}(GSE)$. The bootstrap fraction decreases from 45% using [5] to 37% using [6] being identified as a significant source of error. An increase of Z_{eff} from 1.5 to 2.0 results in a 6% reduction of I_{BS} and a corresponding increase of $I_{ohm}(CDE)$ by 2-3% which is marginal significant. Simultaneously $I_{ohm}(GSE)$ decreases by a significant amount ($\approx 20\%$) improving consistency.

Summarising, the ohmic current is calculated and successfully validated with different methods evaluating the equilibrium evolution solving the CDE and the GSE for an ohmic plasma. A non-inductive plasma with its small ohmic contribution allows to study the sensitivity of the bootstrap model, trapped fraction model, Z_{eff}, and the influence of mis-specified fast particle distributions in I_{NBCD}.

References

[1] R. Fischer, A. Bock, M. Dunne, J.C. Fuchs, L. Giannone, K. Lackner, P.J. McCarthy, E. Poli, R. Preuss, M. Rampp, M. Schubert, J. Stober, W. Suttrop, G. Tardini, M. Weiland, and ASDEX Upgrade Team. Coupling of the flux diffusion equation with the equilibrium reconstruction at ASDEX Upgrade. *Fusion Sci. Technol.*, 69:526–536, 2016.

[2] R. Fischer, A. Bock, A. Burckhart, M. Dunne, O. Ford, J.C. Fuchs, L. Giannone, A. Gude, V. Igochine, A. Lebschy, M. Maraschek, P.J. McCarthy, A. Mlynek, A. Snicker, J. Stober, G. Tardini, M. Weiland, M. Willensdorfer, and ASDEX Upgrade Team. Upgraded equilibrium reconstruction by coupling of an extended set of measurements with current diffusion modelling at asdex upgrade. In *43th EPS Conference on Plasma Physics*, page P1.016. European Physical Society, Geneva, 2016.

[3] L. Giannone et al. In *44th EPS Conference on Plasma Physics*, page P5.133. European Physical Society, Geneva, 2017.

[4] Y. R. Lin-Liu and R. L. Miller. Upper and lower bounds of the effective trapped particle fraction in general tokamak equilibria. *Physics of Plasmas*, 2:1666, 1995.

[5] O. Sauter, C. Angioni, and Y.R. Lin-Liu. Neoclassical conductivity and bootstrap current formulas for general axisymmetric equilibria and arbitrary collisionality regime. *Physics of Plasmas*, 6:2834, 1999. Erratum: 9:5140, 2002.

[6] R. Hager and C.S. Chang. Gyrokinetic neoclassical study of the bootstrap current in the tokamak edge pedestal with fully non-linear Coulomb collisions. *Physics of Plasmas*, 23:042502, 2016.